Resonance fluorescence quenching and spectral line narrowing via quantum interference in a four-level atom driven by two coherent fields

Fu-li Li[1,2] and Shi-Yao Zhu[1,3]
[1]*Department of Physics, Hong Kong Baptist University, Hong Kong, People's Republic of China*
[2]*Department of Applied Physics, Xian Jiaotong University, Xian 710049, People's Republic of China*
[3]*Department of Physics, Texas A&M University, College Station, Texas 77843*
(Received 23 April 1998; revised manuscript received 31 August 1998)

The resonance fluorescence from a four-level atom driven by two coherent fields is studied. If the dipole moments between the two upper levels and each of the two lower levels are parallel, the spontaneous emission paths from the upper levels to the lower levels will have strongly or even completely destructive quantum interference. We show that this quantum interference will result in a complete inhibition of the fluorescence when one of the driving fields is tuned at the middle point of the upper levels. The quantum interference will lead to the dependence of atomic populations at steady state on the initial condition, when both of the driving fields are tuned to the middle point of the upper levels. When the dipole moments are close to but not exactly parallel, or none of the driving fields is tuned at the middle point of the upper levels and there is a small difference between detunings of the two driving fields to the uppermost level, ultranarrow lines at the spectral center appear because of the destructive quantum interference. [S1050-2947(99)02203-9]

PACS number(s): 42.50.Ct, 42.50.Gy, 32.80.Bx, 42.50.Lc

I. INTRODUCTION

The linear superposition of states is one of fundamental principles of quantum mechanics. It results in various interference phenomena in quantum mechanics. When an atom is initially at a linear superposition of excited states, i.e., atomic coherent state, the probability for transition from the superposition state to a single lower level is given by squaring the dipole moment matrix element between the initial and final states. Since the initial state is a linear superposition of excited levels, the transition probability contains interference terms contributed by different transition pathways between the excited levels to the single lower one. The interference terms can depress the transition. Moreover, under certain conditions the transition may even be totally inhibited via the interference although the excited levels are populated. In recent years, this quantum interference appearing in a multilevel atomic system has attracted a lot of attention because it can lead to absorption cancellation [1–10], electromagnetically induced transparency (EIT) [6–8], and population inversion without emission [2], which have potential applications to a new type of laser system operating without population inversion (LWI) [1–4], transparent high-refraction index materials [11–14], and highly sensitive magnetometers [15]. In particular, it is shown that spontaneous emission of an excited atom in free space can be depressed via the quantum interference in a wide frequency region [16–20]. Therefore, it may become possible to control spontaneous emission of an atom and the corresponding effects via the quantum interference [21]. Studing the influence of quantum interference on spontaneous emission of atoms is becoming a hot subject in the field of quantum optics.

The realization of quantum interference in an atomic system depends on an atomic level configuration. The atomic systems employed in most of existing studies of quantum interference for cancellation of spontaneous emission have a common feature that there is an excited doublet which is coupled by the same vacuum modes to a single lower level. The two transition pathways from the upper levels to the lower one can have quantum interference under certain conditions. It was shown that when the atom is initially in a superposition of the upper levels [16] or the excited doublet is driven by a coherent field to an auxiliary level [17–19], the quantum interference can lead to depression or even cancellation of spontaneous emission from the excited doublet to the lower level. The theoretical prediction was demonstrated in an experiment [20].

Since the incoherent part of resonance fluorescence results from spontaneous emission of a driven atom, it is natural to ask what are the effects of the quantum interference to the resonance fluorescence. By applying a coherent field to the transition from the doublet to the lower level, Cardimona, Raymer, and Stroud showed that the atom can be driven into a dark state in which the fluorescence is totally depressed via the quantum interference regardless of the intensity of the excited laser [22]. In Refs. [23–25], the conclusion was confirmed again, and moreover it was shown that an ultranarrow central peak appears in the resonance fluorescence spectrum when the quantum interference becomes incomplete.

In this paper, we consider a four-level atomic model which was proposed for studying cancellation of spontaneous emission via quantum interference [17]. In previous studies [17–19], the two upper levels are coupled to one of the lower levels by a coherent field and to another level by the vacuum modes. We now apply two coherent fields to transitions between the upper and lower levels. We are interested in the effects of quantum interference to resonance fluorescence spectra of the atom. In contrast to the case stud-

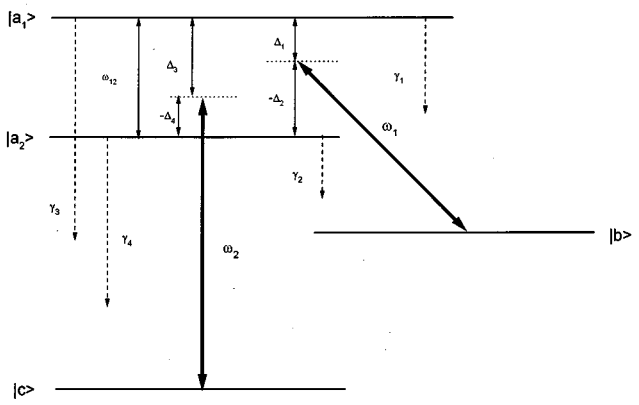

FIG. 1. Level scheme of a model atom.

ied in Refs. [23–25], since there are two coherent driving fields in this model the quantum-interference effects created by the two fields may interact each other. Therefore, it may be possible in the present case by using one of the driving fields to control the resonance fluorescence induced by another one.

As is well known, the spontaneous emission spectrum of an atom can be altered by driving the atom with resonant fields. The resonant fluorescence spectrum for a driven two-level atom develops a three-peak distribution when the driving field is sufficiently strong [26]. The widths and peak heights of resonance fluorescence spectra for a V-type, Λ-type, and cascade three-level atom are strongly affected by driving fields [27,28]. These modifications can be attributed to different reasons such as the driving configuration, atomic parameters, amplitudes of Rabi frequencies of driving fields, and so on [27,28]. Here we want to know, except with those approaches, by use of quantum interference between different spontaneous emission processes how to modify the resonance fluorescence spectra. We will show that the interference can result in many interesting effects such as ultranarrowing central lines and population trapping in the upper levels. Without the interference, these effects completely disappear. One cannot except these results when not considering the interference.

This paper is organized as follows. In Sec. II the model is presented and the formula of the calculation of the fluorescence spectra is developed. In Sec. III we study nondecaying dressed states and total inhibition of the resonance fluorescence. In Sec. IV we show some numerical results of the fluorescence spectra and discuss how the destructive quantum interference leads to the ultranarrowness of the spectra line. The conclusions are summarized in Sec. V.

II. THE MODEL AND THE CALCULATION OF THE FLUORESCENCE SPECTRA

A. Model

The model under consideration has four levels as shown in Fig. 1. The transitions from the upper levels $|a_1\rangle$ with energy $\hbar\omega_{a_1}$ and $|a_2\rangle$ with energy $\hbar\omega_{a_2}$ to the lower-lying levels $|b\rangle$ with energy $\hbar\omega_b$ and $|c\rangle$ with energy $\hbar\omega_c$ are driven by two coherent fields with frequencies ω_1 and ω_2, respectively. These transitions are also coupled by the vacuum modes. If the separations of $|a_1\rangle$ and $|a_2\rangle$ from $|c\rangle$ are much larger than those from $|b\rangle$ or vice versa, we can consider that the vacuum modes coupling $|a_{1,2}\rangle$ to $|b\rangle$ are totally different from those coupling $|a_{1,2}\rangle$ to $|c\rangle$. Meanwhile, we assume that the vacuum modes which couple $|a_1\rangle$ and $|a_2\rangle$ to $|b\rangle$ ($|c\rangle$) are the same. We also assume that the dipole transition between $|b\rangle$ and $|c\rangle$ is forbidden because of the same parity. Detunings shown in Fig. 1 are defined as $\Delta_{1,2}=\omega_{a_{1,2}}-\omega_b-\omega_1$ and $\Delta_{3,4}=\omega_{a_{1,2}}-\omega_c-\omega_2$. With the rotation-wave approximation [29(a)] the model can be described by the Hamiltonian

$$\hat{H}=\hat{H}_0+\hat{V}_{ab}+\hat{V}_{ac}+\hat{V}_{Rb}+\hat{V}_{Rc}, \tag{1}$$

where

$$\hat{H}_0=\hbar\omega_{a_1}|a_1\rangle\langle a_1|+\hbar\omega_{a_2}|a_2\rangle\langle a_2|+\hbar\omega_b|b\rangle\langle b| +\hbar\omega_c|c\rangle\langle c|+\sum_q \hbar\omega_q a_q^\dagger a_q+\sum_k \hbar\omega_k b_k^\dagger b_k, \tag{2}$$

$$\hat{V}_{ab}=\hbar\Omega_1 e^{-i\omega_1 t}|a_1\rangle\langle b|+\hbar\Omega_2 e^{-i\omega_1 t}|a_2\rangle\langle b|+\text{H.c.}, \tag{3}$$

$$\hat{V}_{ac}=\hbar\Omega_3 e^{-i\omega_2 t}|a_1\rangle\langle c|+\hbar\Omega_4 e^{-i\omega_2 t}|a_2\rangle\langle c|+\text{H.c.}, \tag{4}$$

$$\hat{V}_{Rb}=\hbar\sum_q (g_q^{(1)}a_q|a_1\rangle\langle b|+g_q^{(2)}a_q|a_2\rangle\langle b|+\text{H.c.}), \tag{5}$$

$$\hat{V}_{Rc}=\hbar\sum_k (g_k^{(3)}a_k|a_1\rangle\langle c|+g_k^{(4)}a_k|a_2\rangle\langle c|+\text{H.c.}). \tag{6}$$

In the above equations, Ω_i ($i=1,2,3,4$) are the Rabi frequencies of the coherent fields driving the transitions from the upper levels $|a_{1,2}\rangle$ to the lower-lying levels $|b\rangle$ and $|c\rangle$, which are defined as

$$\Omega_{1,2}=\hbar^{-1}E_1\boldsymbol{\mu}_{a_{1,2};b}\cdot\hat{\mathbf{e}}_1, \tag{7}$$

$$\Omega_{3,4}=\hbar^{-1}E_2\boldsymbol{\mu}_{a_{1,2};c}\cdot\hat{\mathbf{e}}_2, \tag{8}$$

where $E_{1,2}$ and $\hat{\mathbf{e}}_{1,2}$ are the complex amplitudes and polarizations of the two driving fields, respectively. $\boldsymbol{\mu}_{a_{1,2};b}=\langle a_{1,2}|(-e\mathbf{r})|b\rangle$ and $\boldsymbol{\mu}_{a_{1,2};c}=\langle a_{1,2}|(-e\mathbf{r})|c\rangle$ are the matrix elements of the electric dipole moments of the transitions from $|a_{1,2}\rangle$ to $|b\rangle$ and $|c\rangle$, respectively. a_q ($a_q^\dagger$) is the annihilation (creation) operator for the qth mode of the vacuum which couples $|a_{1,2}\rangle$ to $|b\rangle$, and b_k ($b_k^\dagger$) is the annihilation (creation) operator for the kth mode of the vacuum which

couples $|a_{1,2}\rangle$ to $|c\rangle$. $g_q^{(1,2)}$ ($g_k^{(3,4)}$) are the coupling constants between the qth (kth) vacuum mode and the atomic transitions from $|a_{1,2}\rangle$ to $|b\rangle$ ($|c\rangle$).

B. Motion equation of the density matrix

In the interaction picture, the Hamiltonian (1) can be written as

$$\hat{H}_I=\hat{V}_{CI}+\hat{V}_{RI}, \tag{9}$$

where

$$\begin{aligned}\hat{V}_{CI}=&\hbar\Omega_1 e^{i\Delta_1 t}|a_1\rangle\langle b|+\hbar\Omega_2 e^{i\Delta_2 t}|a_2\rangle\langle b|+\text{H.c.}\\&+\hbar\Omega_3 e^{i\Delta_3 t}|a_1\rangle\langle c|+\hbar\Omega_4 e^{i\Delta_4 t}|a_2\rangle\langle c|+\text{H.c.},\end{aligned} \tag{10}$$

$$\begin{aligned}\hat{V}_{RI}=&\hbar\sum_q\,(g_q^{(1)}e^{i\Delta_{1q}t}a_q|a_1\rangle\langle b|\\&+g_q^{(2)}e^{i\Delta_{2q}t}a_q|a_2\rangle\langle b|+\text{H.c.})\\&+\hbar\sum_k\,(g_k^{(3)}e^{i\Delta_{1k}t}a_k|a_1\rangle\langle c|\\&+g_k^{(4)}e^{i\Delta_{2k}t}a_k|a_2\rangle\langle c|+\text{H.c.})\end{aligned} \tag{11}$$

with $\Delta_{1q}=\omega_{a_1}-\omega_b-\omega_q$, $\Delta_{2q}=\omega_{a_2}-\omega_b-\omega_q$, $\Delta_{1k}=\omega_{a_1}-\omega_c-\omega_k$, and $\Delta_{2k}=\omega_{a_2}-\omega_c-\omega_k$. According to the generalized reservior theory with the Weisskopf-Wigner approximation [29(b)], we can derive the equations of motion for the reduced atomic density-matrix elements which are [18,30]

$$\begin{aligned}\dot{\rho}_{a_1a_1}=&-(\gamma_1+\gamma_3)\rho_{a_1a_1}-\tfrac{1}{2}(p_1\sqrt{\gamma_1\gamma_2}+p_2\sqrt{\gamma_3\gamma_4})\\&\times(e^{i\Delta t}\rho_{a_2a_1}+e^{-i\Delta t}\rho_{a_1a_2})-i\Omega_1 e^{i\Delta_1 t}\rho_{ba_1}\\&+i\Omega_1^* e^{-i\Delta_1 t}\rho_{a_1b}-i\Omega_3 e^{i\Delta_3 t}\rho_{ca_1}+i\Omega_3^* e^{-i\Delta_3 t}\rho_{a_1c},\end{aligned} \tag{12}$$

$$\begin{aligned}\dot{\rho}_{a_1a_2}=&-\tfrac{1}{2}(\gamma_1+\gamma_2+\gamma_3+\gamma_4)\rho_{a_1a_2}-\tfrac{1}{2}(p_1\sqrt{\gamma_1\gamma_2}\\&+p_2\sqrt{\gamma_3\gamma_4})e^{i\Delta t}(\rho_{a_1a_1}+\rho_{a_2a_2})-i\Omega_1 e^{i\Delta_1 t}\rho_{ba_2}\\&-i\Omega_3 e^{i\Delta_3 t}\rho_{ca_2}+i\Omega_2^* e^{-i\Delta_2 t}\rho_{a_1b}+i\Omega_4^* e^{-i\Delta_4 t}\rho_{a_1c},\end{aligned} \tag{13}$$

$$\begin{aligned}\dot{\rho}_{a_1b}=&-\tfrac{1}{2}(\gamma_1+\gamma_3)\rho_{a_1b}-\tfrac{1}{2}(p_1\sqrt{\gamma_1\gamma_2}\\&+p_2\sqrt{\gamma_3\gamma_4})e^{i\Delta t}\rho_{a_2b}-i\Omega_1 e^{i\Delta_1 t}(\rho_{bb}-\rho_{a_1a_1})\\&+i\Omega_2 e^{i\Delta_2 t}\rho_{a_1a_2}-i\Omega_3 e^{-i\Delta_3 t}\rho_{cb},\end{aligned} \tag{14}$$

$$\begin{aligned}\dot{\rho}_{a_1c}=&-\tfrac{1}{2}(\gamma_1+\gamma_3)\rho_{a_1c}-\tfrac{1}{2}(p_1\sqrt{\gamma_1\gamma_2}\\&+p_2\sqrt{\gamma_3\gamma_4})e^{i\Delta t}\rho_{a_2c}-i\Omega_3 e^{i\Delta_3 t}(1-\rho_{bb}-\rho_{a_2a_2}\\&-2\rho_{a_1a_1})+i\Omega_4 e^{i\Delta_4 t}\rho_{a_1a_2}-i\Omega_1 e^{i\Delta_1 t}\rho_{bc},\end{aligned} \tag{15}$$

$$\begin{aligned}\dot{\rho}_{a_2a_2}=&-(\gamma_2+\gamma_4)\rho_{a_2a_2}-\tfrac{1}{2}(p_1\sqrt{\gamma_1\gamma_2}\\&+p_2\sqrt{\gamma_3\gamma_4})(e^{i\Delta t}\rho_{a_2a_1}+e^{-i\Delta t}\rho_{a_1a_2})\\&-i\Omega_2 e^{i\Delta_2 t}\rho_{ba_2}+i\Omega_2^* e^{-i\Delta_2 t}\rho_{a_2b}\\&-i\Omega_4 e^{i\Delta_4 t}\rho_{ca_2}+i\Omega_4^* e^{-i\Delta_4 t}\rho_{a_2c},\end{aligned} \tag{16}$$

$$\begin{aligned}\dot{\rho}_{a_2b}=&-\tfrac{1}{2}(\gamma_2+\gamma_4)\rho_{a_2b}-\tfrac{1}{2}(p_1\sqrt{\gamma_1\gamma_2}\\&+p_2\sqrt{\gamma_3\gamma_4})e^{-i\Delta t}\rho_{a_1b}-i\Omega_2 e^{i\Delta_2 t}(\rho_{bb}-\rho_{a_2a_2})\\&+i\Omega_1 e^{i\Delta_1 t}\rho_{a_2a_1}-i\Omega_4 e^{i\Delta_4 t}\rho_{cb},\end{aligned} \tag{17}$$

$$\begin{aligned}\dot{\rho}_{a_2c}=&-\tfrac{1}{2}(\gamma_2+\gamma_4)\rho_{a_2c}-\tfrac{1}{2}(p_1\sqrt{\gamma_1\gamma_2}\\&+p_2\sqrt{\gamma_3\gamma_4})e^{-i\Delta t}\rho_{a_1c}-i\Omega_4 e^{i\Delta_4 t}\\&\times(1-\rho_{bb}-\rho_{a_1a_1}-2\rho_{a_2a_2})\\&+i\Omega_3 e^{i\Delta_3 t}\rho_{a_2a_1}-i\Omega_2 e^{i\Delta_2 t}\rho_{bc},\end{aligned} \tag{18}$$

$$\begin{aligned}\dot{\rho}_{bb}=&\gamma_1\rho_{a_1a_1}+\gamma_2\rho_{a_2a_2}+p_1\sqrt{\gamma_1\gamma_2}(e^{-i\Delta t}\rho_{a_1a_2}\\&+e^{i\Delta t}\rho_{a_2a_1})+i\Omega_1 e^{i\Delta_1 t}\rho_{ba_1}-i\Omega_1^* e^{-i\Delta_1 t}\rho_{a_1b}\\&+i\Omega_2 e^{i\Delta_2 t}\rho_{ba_2}-i\Omega_2^* e^{-i\Delta_2 t}\rho_{a_2b},\end{aligned} \tag{19}$$

$$\begin{aligned}\dot{\rho}_{bc}=&-i\Omega_1^* e^{-i\Delta_1 t}\rho_{a_1c}-i\Omega_2^* e^{-i\Delta_2 t}\rho_{a_2c}\\&+i\Omega_3 e^{i\Delta_3 t}\rho_{ba_1}+i\Omega_4 e^{i\Delta_4 t}\rho_{ba_2}.\end{aligned} \tag{20}$$

When arriving at Eqs. (12)–(20), we have used the normalization condition $\rho_{a_1a_1}+\rho_{a_2a_2}+\rho_{bb}+\rho_{cc}=1$ to replace ρ_{cc}. In the above equations, γ_1, γ_2, γ_3, and γ_4 are the spontaneous decay rates from the two upper levels to the lower levels given by $\gamma_{1,2}=|\boldsymbol{\mu}_{a_{1,2};b}|^2(\omega_{a_{1,2}}-\omega_b)^3/3\pi\epsilon_0\hbar c^3$ and $\gamma_{3,4}=|\boldsymbol{\mu}_{a_{1,2};c}|^2(\omega_{a_{1,2}}-\omega_c)^3/3\pi\epsilon_0\hbar c^3$. When deriving Eqs. (12)–(20) by use of the generalized reservior theory [29(b)], we have the crossing terms $\Sigma_q(g_q^{(1)})^*g_q^{(2)}$ and $\Sigma_k(g_k^{(3)})^*g_k^{(4)}$. With the Weisskopf-Wigner approximation, these crossing terms can easily be written as $\boldsymbol{\mu}_{a_1b}\cdot\boldsymbol{\mu}_{a_2b}(\omega_{a_{1,2}}-\omega_b)^3/3\pi\epsilon_0\hbar c^3$ and $\boldsymbol{\mu}_{a_1c}\cdot\boldsymbol{\mu}_{a_2c}(\omega_{a_{1,2}}-\omega_c)^3/3\pi\epsilon_0\hbar c^3$, respectively. Considering that the upper level separation $\Delta=\omega_{12}$ is much smaller than the optical transition frequencies $\omega_{a_{1,2}}-\omega_b$ and $\omega_{a_{1,2}}-\omega_c$, we have replaced these terms by $p_1\sqrt{\gamma_1\gamma_2}$ and $p_2\sqrt{\gamma_3\gamma_4}$, respectively, where $p_{1,2}$ are the alignments of the matrix elements of the dipole moments and are given by

$$p_{1,2}=\frac{\boldsymbol{\mu}_{a_1;b,c}\cdot\boldsymbol{\mu}_{a_2;b,c}}{|\boldsymbol{\mu}_{a_1;b,c}||\boldsymbol{\mu}_{a_2;b,c}|}. \tag{21}$$

In Eqs. (12)–(20), the term $p_1\sqrt{\gamma_1\gamma_2}$ ($p_2\sqrt{\gamma_3\gamma_4}$) represents the effect of quantum interference between the spontaneous-emission pathways from $|a_1\rangle$ to $|b\rangle$ ($|c\rangle$) and from $|a_2\rangle$ to $|b\rangle$ ($|c\rangle$). It reflects the fact that as the atom

decays from the excited sublevel $|a_1\rangle$, it drives the other excited sublevel $|a_2\rangle$ and vice versa because of atomic coherence between $|a_1\rangle$ and $|a_2\rangle$, which is created by the driving fields. We notice that in the above equations the usual decay terms proportional to $\gamma_{1,2}$ and $\gamma_{3,4}$ are always paired with the decay interference terms proportional to $p_1\sqrt{\gamma_1\gamma_2}$ and $p_2\sqrt{\gamma_3\gamma_4}$, respectively, as long as $p_1\neq 0$ and $p_2\neq 0$. They may cancel each other. We will show that under certain conditions the spontaneous emission pathways from $|a_1\rangle$ to $|b\rangle$ ($|c\rangle$) and from $|a_2\rangle$ to $|b\rangle$ ($|c\rangle$) display a destructive interference and the cancellation really happens, which has the atom decouple from the vacuum modes and the fluorescence depressed.

The explicit time-dependent factors of the complex exponential in Eqs. (12)–(20) can be removed with the transformation

$$\Psi_1=e^{-i\Delta_1 t}\rho_{a_1b},\quad \Psi_9=\Psi_1^*, \tag{22}$$

$$\Psi_2=e^{-i\Delta_2 t}\rho_{a_2b},\quad \Psi_{10}=\Psi_2^*, \tag{23}$$

$$\Psi_3=e^{-i\Delta_3 t}\rho_{a_1c},\quad \Psi_{11}=\Psi_3^*, \tag{24}$$

$$\Psi_4=e^{-i\Delta_4 t}\rho_{a_2c},\quad \Psi_{12}=\Psi_4^*, \tag{25}$$

$$\Psi_5=e^{-i\Delta t}\rho_{a_1a_2},\quad \Psi_{13}=\Psi_5^*, \tag{26}$$

$$\Psi_{14}=e^{-i(\Delta_3-\Delta_1)t}\rho_{bc},\quad \Psi_{15}=\Psi_{14}^*, \tag{27}$$

$$\Psi_6=\rho_{a_1a_1},\quad \Psi_7=\rho_{a_2a_2},\quad \Psi_8=\rho_{bb}. \tag{28}$$

Substituting Eqs. (22)–(28) into Eqs. (12)–(20), we can write Eqs. (12)–(20) in the compact vector form [27,28]

$$\frac{d}{dt}\hat{\Psi}=\hat{L}\hat{\Psi}+\hat{I}, \tag{29}$$

where $\hat{\Psi}$ is a column vector whose ith component is Ψ_i and the inhomogeneous term $\hat{I}$ is also a column vector with the nonzero components

$$\hat{I}_3=-i\Omega_3,\quad \hat{I}_{11}=\hat{I}_3^*,\quad \hat{I}_4=-i\Omega_4,\quad \hat{I}_{12}=\hat{I}_4^*. \tag{30}$$

In Eq. (29), $\hat{L}$ is a 15×15 matrix whose explicit expression can be easily derived from Eqs. (12)–(20). Since matrix elements of $\hat{L}$ are time-independent, Eq. (29) is a set of linear first-order differential equations with constant coefficients. Therefore, it has the formal solution

$$\hat{\Psi}(t+\tau)=e^{\tau\hat{L}}\hat{\Psi}(t)+\hat{L}^{-1}[e^{\tau\hat{L}}-1]\hat{I} \tag{31}$$

and the steady-state solution

$$\hat{\Psi}(\infty)=-\hat{L}^{-1}\hat{I}. \tag{32}$$

C. The calculation of the spectra

The model under consideration involves the two driving fields with quite different carrier frequencies. In this way, each field induces its own atomic polarization, which generates its own scattering field. The correlation between the two fields can be neglected. That is to say, the atomic polarizations induced by the two driving fields can be considered separately.

In the interaction picture, the negative-frequency parts of the polarization operators are written as

$$\hat{\mathbf{P}}_{\omega_1}^{(-)}(t)=\boldsymbol{\mu}_{a_1b}e^{i(\omega_{a_1}-\omega_b)t}|a_1\rangle\langle b|+\boldsymbol{\mu}_{a_2b}e^{i(\omega_{a_2}-\omega_b)t}|a_2\rangle\langle b|, \tag{33}$$

$$\hat{\mathbf{P}}_{\omega_2}^{(-)}(t)=\boldsymbol{\mu}_{a_1c}e^{i(\omega_{a_1}-\omega_c)t}|a_1\rangle\langle c|+\boldsymbol{\mu}_{a_2c}e^{i(\omega_{a_2}-\omega_c)t}|a_2\rangle\langle c|, \tag{34}$$

and the positive-frequency parts are

$$\hat{\mathbf{P}}_{\omega_1}^{(+)}(t)=[\hat{\mathbf{P}}_{\omega_1}^{(-)}(t)]^*,\quad \hat{\mathbf{P}}_{\omega_2}^{(+)}(t)=[\hat{\mathbf{P}}_{\omega_2}^{(-)}(t)]^*. \tag{35}$$

In the above, the indices ω_1 and ω_2 obviously refer to the two driving fields. Using the transformations defined in Eqs. (22)–(28) and the formal solution (31), we obtain the single-time expectation values of $\hat{\mathbf{P}}_{\omega_1}^{(-)}(t)$ and $\hat{\mathbf{P}}_{\omega_2}^{(-)}(t)$, which are

$$\begin{aligned}\langle\hat{\mathbf{P}}_{\omega_1}^{(-)}(t+\tau)\rangle=&e^{i(t+\tau)\omega_1}\boldsymbol{\mu}_{a_1b}\sum_{j=1}^{15}\{(e^{\tau\hat{L}})_{9,j}\Psi_j(t)\\&+[\hat{L}^{-1}(e^{\tau\hat{L}}-1)]_{9,j}\hat{I}_j\}\\&+e^{i(t+\tau)\omega_1}\boldsymbol{\mu}_{a_2b}\sum_{j=1}^{15}\{(e^{\tau\hat{L}})_{10,j}\Psi_j(t)\\&+[\hat{L}^{-1}(e^{\tau\hat{L}}-1)]_{10,j}\hat{I}_j\},\end{aligned} \tag{36}$$

$$\begin{aligned}\langle\hat{\mathbf{P}}_{\omega_2}^{(-)}(t+\tau)\rangle=&e^{i(t+\tau)\omega_2}\boldsymbol{\mu}_{a_1c}\sum_{j=1}^{15}\{(e^{\tau\hat{L}})_{11,j}\\&\times\Psi_j(t)+[\hat{L}^{-1}(e^{\tau\hat{L}}-1)]_{11,j}\hat{I}_j\}\\&+e^{i(t+\tau)\omega_2}\boldsymbol{\mu}_{a_2c}\sum_{j=1}^{15}\{(e^{\tau\hat{L}})_{12,j}\Psi_j(t)\\&+[\hat{L}^{-1}(e^{\tau\hat{L}}-1)]_{12,j}\hat{I}_j\}.\end{aligned} \tag{37}$$

With the help of the quantum regression theorem [31], the two-time expectation values of Eqs. (33)–(35) can be written as

$$\langle \hat{\mathbf{P}}^{(-)}_{\omega_1}(t+\tau)\cdot\hat{\mathbf{P}}^{(+)}_{\omega_1}(t)\rangle = e^{i\tau\omega_1}|\boldsymbol{\mu}_{a_1b}|^2\Big((e^{\tau\hat{L}})_{9,9}\Psi_6(t)+(e^{\tau\hat{L}})_{9,8}\Psi_1(t)+(e^{\tau\hat{L}})_{9,10}\Psi_5(t)$$
$$+(e^{\tau\hat{L}})_{9,14}\Psi_3(t)+\sum_{j=1}^{15}[\hat{L}^{-1}(e^{\tau\hat{L}}-1)]_{9,j}\hat{I}_j\Psi_1(t)\Big)+e^{i\tau\omega_1}\boldsymbol{\mu}_{a_1b}\cdot\boldsymbol{\mu}_{ba_2}\Big((e^{\tau\hat{L}})_{9,9}\Psi_{13}(t)$$
$$+(e^{\tau\hat{L}})_{9,8}\Psi_2(t)+(e^{\tau\hat{L}})_{9,10}\Psi_7(t)+(e^{\tau\hat{L}})_{9,14}\Psi_4(t)+\sum_{j=1}^{15}[\hat{L}^{-1}(e^{\tau\hat{L}}-1)]_{9,j}\hat{I}_j\Psi_2(t)\Big)$$
$$+e^{i\tau\omega_1}\boldsymbol{\mu}_{a_2b}\cdot\boldsymbol{\mu}_{ba_1}\Big((e^{\tau\hat{L}})_{10,9}\Psi_6(t)+(e^{\tau\hat{L}})_{10,8}\Psi_1(t)+(e^{\tau\hat{L}})_{10,10}\Psi_5+(e^{\tau\hat{L}})_{10,14}\Psi_3(t)$$
$$+\sum_{j=1}^{15}[\hat{L}^{-1}(e^{\tau\hat{L}}-1)]_{10,j}\hat{I}_j\Psi_1(t)\Big)+e^{i\tau\omega_1}|\boldsymbol{\mu}_{a_2b}|^2\Big((e^{\tau\hat{L}})_{10,9}\Psi_{13}(t)+(e^{\tau\hat{L}})_{10,8}\Psi_2(t)$$
$$+(e^{\tau\hat{L}})_{10,10}\Psi_7(t)+(e^{\tau\hat{L}})_{10,14}\Psi_4(t)+\sum_{j=1}^{15}[\hat{L}^{-1}(e^{\tau\hat{L}}-1)]_{10,j}\hat{I}_j\Psi_2(t)\Big), \tag{38}$$

$$\langle \hat{\mathbf{P}}^{(-)}_{\omega_2}(t+\tau)\cdot\hat{\mathbf{P}}^{(+)}_{\omega_2}(t)\rangle = e^{i\tau\omega_2}|\boldsymbol{\mu}_{a_1c}|^2\Big((e^{\tau\hat{L}})_{11,11}\Psi_6(t)+(e^{\tau\hat{L}})_{11,12}\Psi_5(t)+(e^{\tau\hat{L}})_{11,15}\Psi_1(t)$$
$$+\sum_{j=1}^{15}[\hat{L}^{-1}(e^{\tau\hat{L}}-1)]_{11,j}\hat{I}_j\Psi_3(t)\Big)+e^{i\tau\omega_2}\boldsymbol{\mu}_{a_1c}\cdot\boldsymbol{\mu}_{ca_2}\Big((e^{\tau\hat{L}})_{11,11}\Psi_{13}(t)+(e^{\tau\hat{L}})_{11,12}\Psi_7(t)$$
$$+(e^{\tau\hat{L}})_{11,15}\Psi_2(t)+\sum_{j=1}^{15}[\hat{L}^{-1}(e^{\tau\hat{L}}-1)]_{11,j}\hat{I}_j\Psi_4(t)\Big)+e^{i\tau\omega_2}\boldsymbol{\mu}_{a_2c}\cdot\boldsymbol{\mu}_{ca_1}\Big((e^{\tau\hat{L}})_{12,11}\Psi_6(t)$$
$$+(e^{\tau\hat{L}})_{12,12}\Psi_5(t)+(e^{\tau\hat{L}})_{12,15}\Psi_1(t)+\sum_{j=1}^{15}[\hat{L}^{-1}(e^{\tau\hat{L}}-1)]_{12,j}\hat{I}_j\Psi_3(t)\Big)+e^{i\tau\omega_1}|\boldsymbol{\mu}_{a_2c}|^2$$
$$\times\Big((e^{\tau\hat{L}})_{12,11}\Psi_{13}(t)+(e^{\tau\hat{L}})_{12,12}\Psi_7(t)+(e^{\tau\hat{L}})_{12,15}\Psi_2(t)+\sum_{j=1}^{15}[\hat{L}^{-1}(e^{\tau\hat{L}}-1)]_{12,j}\hat{I}_j\Psi_4(t)\Big). \tag{39}$$

Taking the Fourier transformations of Eqs. (38) and (39), in the limit $t\to\infty$, we find the incoherent fluorescence spectra in the forms [27,28]

$$S^{(1,2)}(\omega)=\mathrm{Re}\,\hat{\Gamma}^{(1,2)}(Z)|_{Z=i\omega}, \tag{40}$$

where

$$\hat{\Gamma}^{(1)}_{\omega_1}(Z)=|\boldsymbol{\mu}_{a_1b}|^2\Big(\hat{M}_{9,9}(Z_1)\Psi_6(\infty)+\hat{M}_{9,10}(Z_1)\Psi_5(\infty)+\hat{M}_{9,14}(Z_1)\Psi_3(\infty)+\hat{M}_{9,8}(Z_1)\Psi_1(\infty)+\sum_{j=1}^{15}\hat{N}_{9,j}(Z_1)\hat{I}_j\Psi_1(\infty)\Big)$$
$$+\boldsymbol{\mu}_{a_1b}\cdot\boldsymbol{\mu}_{ba_2}\Big(\hat{M}_{9,9}(Z_1)\Psi_{13}(\infty)+\hat{M}_{9,10}(Z_1)\Psi_7(\infty)+\hat{M}_{9,14}(Z_1)\Psi_4(\infty)+\hat{M}_{9,8}(Z_1)\Psi_2(\infty)+\sum_{j=1}^{15}\hat{N}_{9,j}(Z_1)\hat{I}_j\Psi_2(\infty)\Big)$$
$$+\boldsymbol{\mu}_{a_2b}\cdot\boldsymbol{\mu}_{ba_1}\Big(\hat{M}_{10,9}(Z_1)\Psi_6(\infty)+\hat{M}_{10,10}(Z_1)\Psi_5(\infty)+\hat{M}_{9,14}(Z_1)\Psi_3(\infty)+\hat{M}_{10,8}(Z_1)\Psi_1(\infty)$$
$$+\sum_{j=1}^{15}\hat{N}_{10,j}(Z_1)\hat{I}_j\Psi_1(\infty)\Big)+|\boldsymbol{\mu}_{a_2b}|^2\Big(\hat{M}_{10,9}(Z_1)\Psi_{13}(\infty)+\hat{M}_{10,10}(Z_1)\Psi_7(\infty)+\hat{M}_{10,14}(Z_1)\Psi_4(\infty)$$
$$+\hat{M}_{10,8}(Z_1)\Psi_2(\infty)+\sum_{j=1}^{15}\hat{N}_{10,j}(Z_1)\hat{I}_j\Psi_2(\infty)\Big) \tag{41}$$

with $Z_1=Z-i\omega_1$ for the fluorescence light induced by the driving field with frequency ω_1 and

$$\hat{\Gamma}^{(2)}_{\omega_2}(Z)=|\boldsymbol{\mu}_{a_1c}|^2\left(\hat{M}_{11,11}(Z_2)\Psi_6(\infty)+\hat{M}_{11,12}(Z_2)\Psi_5(\infty)+\hat{M}_{11,15}(Z_2)\Psi_1(\infty)+\sum_{j=1}^{15}\hat{N}_{11,j}(Z_2)\hat{I}_j\Psi_3(\infty)\right)$$
$$+\boldsymbol{\mu}_{a_1c}\cdot\boldsymbol{\mu}_{ca_2}\left(\hat{M}_{11,11}(Z_2)\Psi_{13}(\infty)+\hat{M}_{11,12}(Z_2)\Psi_7(\infty)+\hat{M}_{11,15}(Z_2)\Psi_2(\infty)+\sum_{j=1}^{15}\hat{N}_{11,j}(Z_2)\hat{I}_j\Psi_4(\infty)\right)$$
$$+\boldsymbol{\mu}_{a_2c}\cdot\boldsymbol{\mu}_{ca_1}\left(\hat{M}_{12,11}(Z_2)\Psi_6(\infty)+\hat{M}_{12,12}(Z_2)\Psi_5(\infty)+\hat{M}_{12,15}(Z_2)\Psi_1(\infty)+\sum_{j=1}^{15}\hat{N}_{12,j}(Z_2)\hat{I}_j\Psi_3(\infty)\right)$$
$$+|\boldsymbol{\mu}_{a_2c}|^2\left(\hat{M}_{12,11}(Z_2)\Psi_{13}(\infty)+\hat{M}_{12,12}(Z_2)\Psi_7(\infty)+\hat{M}_{12,15}(Z_2)\Psi_2(\infty)+\sum_{j=1}^{15}\hat{N}_{12,j}(Z_2)\hat{I}_j\Psi_4(\infty)\right) \quad (42)$$

with $Z_2=Z-i\omega_2$ for the fluorescence light induced by the driving field with frequency ω_2. The matrices $\hat{M}$ and $\hat{N}$ in Eqs. (41) and (42) are defined as

$$\hat{M}(Z)=(Z-\hat{L})^{-1}, \quad (43)$$

$$\hat{N}(Z)=\hat{L}^{-1}\hat{M}(Z). \quad (44)$$

III. QUENCHING STATES OF FLUORESCENCE

Although the fluorescence spectra can numerically be calculated according to the formula developed in the preceding section, we have to come into the atomic dressed-state representation in order to get some physical insights from the numerical results. In this section, we consider the model in the atomic dressed-state representation and show that there are some states in which the fluorescence is totally quenched because of the destructive quantum interference between the spontaneous-emission pathways from $|a_1\rangle$ and $|a_2\rangle$ to $|b\rangle,|c\rangle$.

To remove the time-dependent exponentials in the coherent driving parts of the Hamiltonian (1), we perform the rotation transformation $\exp(-i\hbar^{-1}\hat{H}_d t)$ to the system under consideration, where

$$\hat{H}_d=\hbar(\omega_b+\omega_1)(|a_1\rangle\langle a_1|+|a_2\rangle\langle a_2|)+\hbar\omega_b|b\rangle\langle b|$$
$$+\hbar(\omega_b+\omega_1-\omega_2)|c\rangle\langle c|+\sum_q\hbar\omega_q a_q^\dagger a_q$$
$$+\sum_k\hbar\omega_k b_k^\dagger b_k. \quad (45)$$

In the rotated frame, the Hamiltonian of the system takes the form

$$\hat{H}'=\hat{H}'_b+\hat{V}'_c+\hat{V}'_R, \quad (46)$$

where

$$\hat{H}'_b=\hbar\Delta_1|a_1\rangle\langle a_1|+\hbar\Delta_2|a_2\rangle\langle a_2|+\hbar(\Delta_1-\Delta_3)|c\rangle\langle c|, \quad (47)$$

$$\hat{V}'_c=\hbar\Omega_1|a_1\rangle\langle b|+\hbar\Omega_2|a_2\rangle\langle b|+\text{H.c.},$$
$$+\hbar\Omega_3|a_1\rangle\langle c|+\hbar\Omega_4|a_2\rangle\langle c|+\text{H.c.}, \quad (48)$$

$$\hat{V}'_R=\hbar\sum_q e^{i(\omega_1-\omega_q)t}[g_q^{(1)}a_q|a_1\rangle\langle b|+g_q^{(2)}a_q|a_1\rangle\langle b|]+\text{H.c.}$$
$$+\hbar\sum_k e^{i(\omega_2-\omega_k)t}[g_k^{(3)}a_k|a_1\rangle\langle c|+g_k^{(4)}a_k|a_1\rangle\langle c|]+\text{H.c.} \quad (49)$$

Now $\hat{H}'_b$ and $\hat{V}'_c$ are time-independent. The eigenvectors of $\hat{H}'_b$, i.e., the bare atomic states $|a_{1,2}\rangle$, $|b\rangle$, and $|c\rangle$, define the bare atomic-state representation. The eigenvectors of $\hat{H}'_b+\hat{V}'_c$ constitute the atomic dressed-state representation.

Let us consider the eigenequation

$$(\hat{H}'_b+\hat{V}'_c)|\varphi_\sigma\rangle=\varepsilon_\sigma|\varphi_\sigma\rangle, \quad (50)$$

where

$$|\varphi_\sigma\rangle=C_{1\sigma}|a_1\rangle+C_{2\sigma}|a_2\rangle+C_{3\sigma}|b\rangle+C_{4\sigma}|c\rangle \quad (51)$$

with the integer σ (=1,2,3,4) to label the four eigenvectors (dressed states). The matrix form of Eq. (50) is

$$\begin{pmatrix}\hbar\Delta_1-\varepsilon_\sigma & 0 & \hbar\Omega_1 & \hbar\Omega_3\\ 0 & \hbar\Delta_2-\varepsilon_\sigma & \hbar\Omega_2 & \hbar\Omega_4\\ \hbar\Omega_1 & \hbar\Omega_2 & -\varepsilon_\sigma & 0\\ \hbar\Omega_3 & \hbar\Omega_4 & 0 & \hbar(\Delta_1-\Delta_3)-\varepsilon_\sigma\end{pmatrix}\times\begin{pmatrix}C_{1\sigma}\\ C_{2\sigma}\\ C_{3\sigma}\\ C_{4\sigma}\end{pmatrix}=0. \quad (52)$$

In the following discussions, we assume $\Omega_1=\Omega_2$ and $\Omega_3=\Omega_4$. To the model under consideration, we believe that these assumptions will not bring serious restrictions to our conclusions. For Eq. (52), we find that there are several special cases in which the analytical solutions can be obtained.

(i) When $\Delta_1=\omega_{12}/2\equiv\Delta_s$ but $\Delta_3\neq\Delta_s$, one of the eigenvalues for Eq. (52) is $\varepsilon_0=0$, and the corresponding eigenvector (dressed state) is

$$|\varphi_I\rangle=\frac{1}{\sqrt{2\Omega_1^2+\Delta_s^2}}[-\Omega_1|a_1\rangle+\Omega_1|a_2\rangle+\Delta_s|b\rangle]. \quad (53)$$

(ii) For the opposite case, when $\Delta_3=\Delta_s$ but $\Delta_1\neq\Delta_s$, Eq. (52) has the eigenvector (dressed state)

$$|\varphi_{II}\rangle=\frac{1}{\sqrt{2\Omega_3^2+\Delta_s^2}}[-\Omega_3|a_1\rangle+\Omega_3|a_2\rangle+\Delta_s|c\rangle] \quad (54)$$

with the eigenvalue $\varepsilon_0=0$.

(iii) When $\Delta_1=\Delta_3\neq\Delta_s$, Eq. (52) has the eigenvector (dressed state)

$$|\varphi_{III}\rangle=\frac{1}{\sqrt{\Omega_1^2+\Omega_3^2}}[\Omega_3|b\rangle-\Omega_1|c\rangle] \quad (55)$$

with the eigenvalue $\varepsilon_0=0$.

(iv) When $\Delta_1=\Delta_3=\Delta_s$, we have a twofold degeneracy for the eigenvalue, $\varepsilon_0=0$. The two eigenvectors (dressed states) are

$$|\varphi_{IV}\rangle=|\varphi_{III}\rangle, \quad (56)$$

$$|\varphi_V\rangle=\left(\frac{\Omega_1^2+\Omega_3^2}{2(\Omega_1^2+\Omega_3^2)+\Delta_s^2}\right)^{1/2}\times\left[|a_1\rangle-|a_2\rangle-\frac{\Delta_s}{\Omega_1^2+\Omega_3^2}(\Omega_1|b\rangle+\Omega_3|c\rangle)\right]. \quad (57)$$

We shall show that under certain conditions the resonance fluorescence can be totally inhibited because of these atomic dressed states.

From the point of view of physics, the resonance fluorescence emitted from an atom which is driven by coherent fields results from the transitions between the atomic dressed states in vacuum. The fluorescence with frequency $\omega-\hbar^{-1}(\varepsilon_{\sigma'}-\varepsilon_\sigma)$ is generated by the transition from $|\varphi_\sigma\rangle$ to $|\varphi_{\sigma'}\rangle$, and its emission rate is proportional to $|\langle\varphi_{\sigma'}|\hat{\mathbf{P}}_\omega^{(+)}|\varphi_\sigma\rangle|^2$. From Eqs. (33) and (34), for the emission lines with the central frequencies ω_1 and ω_2, we have

$$|\langle\varphi_{\sigma'}|\hat{\mathbf{P}}_{\omega_1}^{(+)}|\varphi_\sigma\rangle|^2=|\boldsymbol{\mu}_{a_1b}|^2[C_{1\sigma}^2+C_{2\sigma}^2+2p_1C_{1\sigma}C_{2\sigma}]C_{3\sigma'}^2, \quad (58)$$

$$|\langle\varphi_{\sigma'}|\hat{\mathbf{P}}_{\omega_2}^{(+)}|\varphi_\sigma\rangle|^2=|\boldsymbol{\mu}_{a_1c}|^2[C_{1\sigma}^2+C_{2\sigma}^2+2p_2C_{1\sigma}C_{2\sigma}]C_{4\sigma'}^2, \quad (59)$$

where we assumed that $|\boldsymbol{\mu}_{a_1b}|=|\boldsymbol{\mu}_{a_2b}|$ and $|\boldsymbol{\mu}_{a_1c}|=|\boldsymbol{\mu}_{a_2c}|$. In the above equations, there are interference terms $2p_1C_{1\sigma}C_{2\sigma}C_{3\sigma'}^2$ and $2p_2C_{1\sigma}C_{2\sigma}C_{4\sigma'}^2$, which result from the decay pathways $|a_1\rangle\rightarrow|b\rangle,|a_2\rangle\rightarrow|b\rangle$ and $|a_1\rangle\rightarrow|c\rangle,|a_2\rangle\rightarrow|c\rangle$, respectively. Since these terms can take negative values and then cancel the first and second terms of Eqs. (58) and (59), the rates may become zero. Therefore, the interference between the decay pathways can depress the transition from $|\varphi_\sigma\rangle$ to $|\varphi_{\sigma'}\rangle$. When $p_1=+1$ or -1 ($\boldsymbol{\mu}_{a_1b}$ and $\boldsymbol{\mu}_{a_2b}$ are parallel or antiparallel) and $p_2=+1$ or -1 ($\boldsymbol{\mu}_{a_1c}$ and $\boldsymbol{\mu}_{a_2c}$ are parallel or antiparallel), the interference effects become maximal. However, the interference effects always exist as long as $p_1\neq0$ and $p_2\neq0$.

From Eqs. (58) and (59), we find that in all four cases mentioned above, the transitions from the dressed states with the eigenvalue $\varepsilon_0=0$ [Eqs. (53)–(57)] to all of the eigenvectors (dressed states) of Eq. (52) can be depressed. It means that these dressed states with the eigenvalue $\varepsilon_0=0$ can become nondecaying in the vacuum. Therefore, when one of the driving fields or both are tuned to the middle point between the two upper levels and the dipole moments are parallel ($p_1=p_2=1$), or the two fields have the same detuning, the atom at steady state will populate at the nondecaying dressed state and consequently the total fluorescence will be completely inhibited.

There are two mechanisms for quenching of the resonance fluorescence. The nondecaying states $|\varphi_I\rangle$, $|\varphi_{II}\rangle$, and $|\varphi_V\rangle$ have a common feature that the amplitudes for the components of $|a_1\rangle$ and $|a_2\rangle$ are same but their signs are opposite. According to the above discussions, this feature suggests that the completely destructive interference between the two decay pathways takes place in the transitions from $|\varphi_I\rangle$, $|\varphi_{II}\rangle$, and $|\varphi_V\rangle$ to any dressed states, when the dipole moments are parallel. Therefore, the destructive quantum interference between the spontaneous emission pathways results in the total fluorescence inhibition, when the system enters one of these nondecaying states.

On the other hand, there is no upper-level component in the dressed state $|\varphi_{III}\rangle$ ($|\varphi_{IV}\rangle$). Therefore, when the atom is in $|\varphi_{III}\rangle$ ($|\varphi_{IV}\rangle$), no spontaneous emission happens and no fluorescence appears. Obviously, the disappearance of fluorescence does not result from the destructive interference between the spontaneous-emission pathways. In fact, the destructive interference between the absorption pathways from $|b\rangle$ to $|a_{1,2}\rangle$ and from $|c\rangle$ to $|a_{1,2}\rangle$ leads to the population trapping in the lower levels and the disappearance of fluorescence [32(a)]. In the Λ configuration of a three-level atom, there also exists this kind of inhibition fluorescence phenomenon (lower-level trapping) [27].

In the case of $\Delta_1=\Delta_3=\omega_{12}/2$, however, the two mechanisms may play their roles simultaneously and the system can stay in $|\varphi_I\rangle$, $|\varphi_{II}\rangle$, $|\varphi_{IV}\rangle$, or $|\varphi_V\rangle$, or even in a superposition of $|\varphi_{IV}\rangle$ and $|\varphi_V\rangle$.

We can examine the above conclusions in a direct way. In the rotated frame, when the atom is in the dressed state $|\varphi_\sigma\rangle$, the corresponding density-matrix operator is $|\varphi_\sigma\rangle\langle\varphi_\sigma|$. In the interaction picture, the density-matrix operator is given by

$$\hat{\rho}_I=\exp[i\hbar^{-1}(\hat{H}_0-\hat{H}_d)t]|\varphi_\sigma\rangle\langle\varphi_\sigma|\exp[-i\hbar^{-1}(\hat{H}_0-\hat{H}_d)t]. \quad (60)$$

According to definitions (22)–(28), we have

$$\Psi_1(\infty)=\Psi_9(\infty)=C_{1\sigma}C_{3\sigma}, \quad \Psi_2(\infty)=\Psi_{10}(\infty)=C_{2\sigma}C_{3\sigma}, \quad (61)$$

$$\Psi_3(\infty)=\Psi_{11}(\infty)=C_{1\sigma}C_{4\sigma}, \quad \Psi_4(\infty)=\Psi_{12}(\infty)=C_{2\sigma}C_{4\sigma}, \quad (62)$$

$$\Psi_5(\infty)=\Psi_{13}(\infty)=C_{1\sigma}C_{2\sigma},$$

$$\Psi_{14}(\infty)=\Psi_{15}(\infty)=C_{3\sigma}C_{4\sigma}, \tag{63}$$

$$\Psi_6(\infty)=C_{1\sigma}^2, \quad \Psi_7(\infty)=C_{2\sigma}^2, \quad \Psi_8(\infty)=C_{3\sigma}^2. \tag{64}$$

It is easily shown that for $p_1=1$ and $p_2=1$, the column vectors $\hat{\Psi}$ with the components (61)–(64) given by $|\varphi_I\rangle$, $|\varphi_{II}\rangle$, and $|\varphi_V\rangle$ are the steady-state solutions of Eq. (29), if $\Delta_1=\Delta_s$ or $\Delta_3=\Delta_s$, or $\Delta_1=\Delta_3=\Delta_s$ ($\Delta_s=\omega_{12}/2$). It means that under the conditions $p_1=1$, $p_2=1$, and $\Delta_1=\omega_{12}/2$ (or $\Delta_3=\omega_{12}/2$) the atom will certainly take the nondecaying pure dressed state $|\varphi_I\rangle$ (or $|\varphi_{II}\rangle$) as its steady state, no matter whether initially it is in a pure or mixed state. From this result, we see that in Eqs. (12)–(20) the decay interference terms can really cancel the usual decay terms and make the atom decouple from the vacuum modes and stay in the pure dressed state $|\varphi_I\rangle$ (or $|\varphi_{II}\rangle$). On the other hand, the matrix elements of $\hat{V}_{ac}$ (or $\hat{V}_{ab}$) between $|\varphi_I\rangle$ (or $|\varphi_{II}\rangle$) and any dressed state are zero and the driving field with frequency ω_2 (or ω_1) cannot couple $|\varphi_I\rangle$ (or $|\varphi_{II}\rangle$) to any dressed states. Therefore, once the atom is in $|\varphi_I\rangle$ (or $|\varphi_{II}\rangle$) under the conditions $p_1=1$, $p_2=1$, and $\Delta_1=\omega_{12}/2$ (or $\Delta_3=\omega_{12}/2$), varying Δ_3 (or Δ_1) will not create any effects on the atom. This result directly originates from the fact that the amplitudes of $|a_1\rangle$ and $|a_2\rangle$ in $|\varphi_I\rangle$ ($|\varphi_{II}\rangle$) are the same with opposite signs and $|c\rangle$ (or $|b\rangle$) is absent. Therefore, the quantum interference leads to this effect.

When $\Delta_1=\Delta_3=\omega_{12}/2$, the column vector $\hat{\Psi}$ with the components (61)–(64) given by $|\varphi_{III}\rangle$ is the steady-state solution of Eq. (29) whatever p_1 and p_2 are. In this case, starting from any state, the atom will eventually evolve into the pure dressed state $|\varphi_{III}\rangle$. From Eqs. (12)–(20), we see that since $|\varphi_{III}\rangle$ does not have the components of the upper levels, each of the decay terms automatically becomes zero. Therefore, the interference between the spontaneous-emission pathways does not take any roles in this case. As mentioned above, the destructive interference between the absorption processes leads to this result.

When $\Delta_1=\Delta_3=\omega_{12}/2$, the situation becomes slightly complex. If one of p_1 and p_2 or both is zero, the steady state for the atom is always $|\varphi_{IV}\rangle$ whatever the initial state is. If $p_1=p_2=1$, the column vectors $\hat{\Psi}$ for $|\varphi_I\rangle$, $|\varphi_{II}\rangle$, $|\varphi_{IV}\rangle$, $|\varphi_V\rangle$, and the superposition states which take the form $A|\varphi_{IV}\rangle+B|\varphi_V\rangle(AA^*+BB^*=1)$ all satisfy the stationary equation of Eq. (29). It means that these states can all be taken as a candidate of the steady state. Which one will be the steady state depends on the initial condition. Therefore, in this case the quantum interference results in the dependence of the steady state on the initial state.

For a general case, it is not an easy job analytically to find out the eigenvectors and the corresponding eigenvalues for Eq. (52). We have numerically solved Eq. (52) for various parameters. We find that if the four eigenvectors $|\varphi_\sigma\rangle$ of Eq. (52) are numbered from 1 to 4 in terms of the absolute values of their eigenenergies in a decreasing order, the amplitudes of $|a_{1,2}\rangle$ components always have the same sign in $|\varphi_1\rangle$ and $|\varphi_2\rangle$ but the opposite sign in $|\varphi_3\rangle$ and $|\varphi_4\rangle$. Hence, the destructive quantum interference between the decay pathways $|a_1\rangle\rightarrow|b\rangle$ (or $|c\rangle$) and $|a_2\rangle\rightarrow|b\rangle$ (or $|c\rangle$) takes its role only in the transitions from $|\varphi_3\rangle$ and $|\varphi_4\rangle$ to any dressed states when the corresponding dipole moments are parallel. Therefore, the populations in $|\varphi_3\rangle$ and $|\varphi_4\rangle$ at steady state measure the role of the destructive quantum interference, while those in $|\varphi_1\rangle$ and $|\varphi_2\rangle$ at steady state measure the role of the constructive quantum interference.

IV. DISCUSSIONS OF NUMERICAL RESULTS

From the studies of the preceding sections, we have seen that the quantum interference between the spontaneous emission pathways is mainly controlled by the parameters p_1, p_2 and Δ_1, Δ_3. In this section, we shall use the equations developed in Sec. II to show some numerical results for the resonance fluorescence spectra for various values of these parameters. In our calculations, we scaled $(\omega-\omega_{1,2})$ by γ_3 and $S^{(1,2)}(\omega)$ by $|\boldsymbol{\mu}_{a_1b}|^2\gamma_3^{-1}$. The rescaled and dimension-

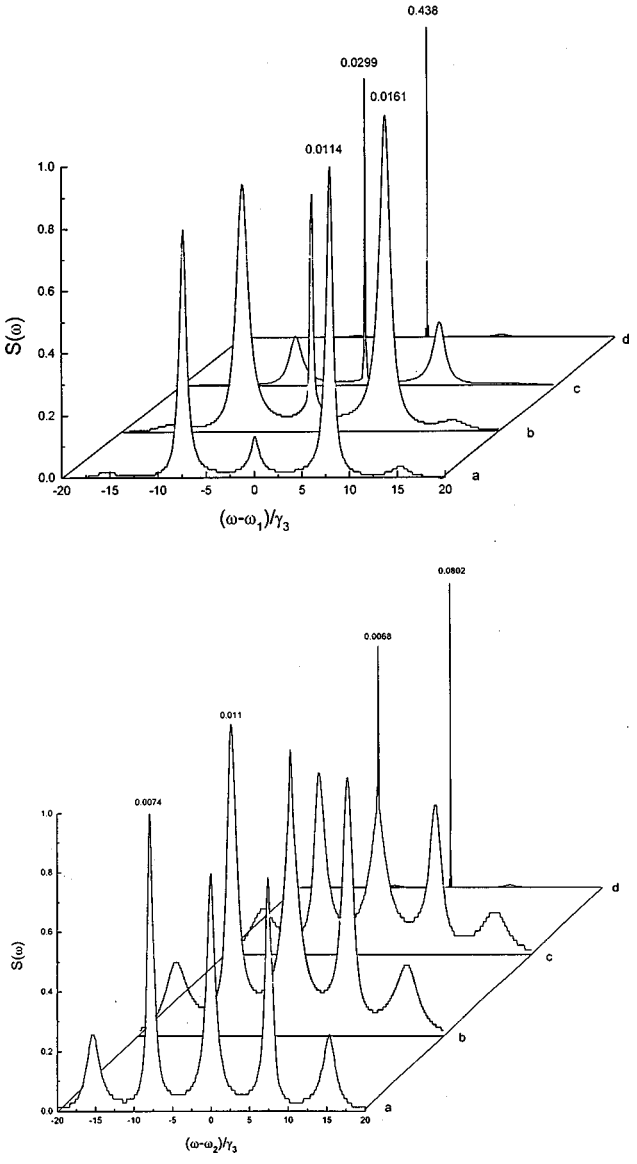

FIG. 2. Resonance fluorescence spectra which is induced by the dipoles (i) $\hat{\mathbf{P}}_{\omega_1}^{(+)}$, (ii) $\hat{\mathbf{P}}_{\omega_2}^{(+)}$ with $\Omega_1=\Omega_2=2.0$, $\Omega_3=\Omega_4=5.0$, $\gamma_1=\gamma_2=0.5$, $\gamma_3=\gamma_4=1.0$, $\omega_{12}=2.0$, $\Delta_1=1.0$, and $\Delta_3=0.0$. (a) $p_1=p_2=0.0$; (b) $p_1=p_2=0.8$; (c) $p_1=p_2=0.99$; (d) $p_1=p_2=0.999$.

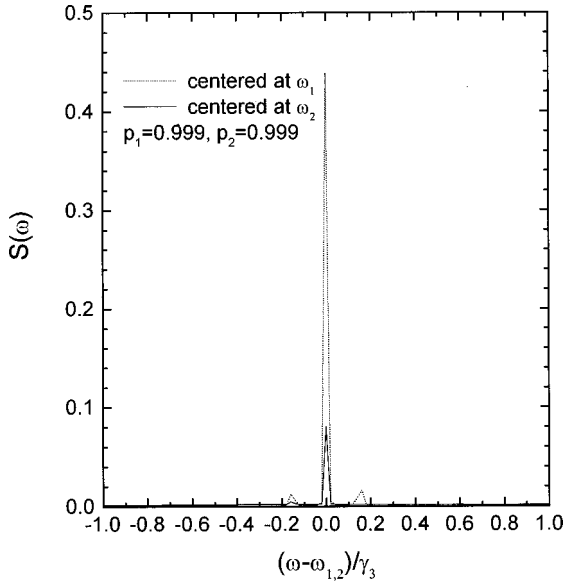

FIG. 3. The detail structure of the curves (d) in Fig. 2.

less spectral intensity is represented by $S(\omega)$ in all the figures. We will also use the dressed states developed in Sec. III to discuss the numerical results and to examine the interference effects. The discussions are based on Eqs. (58) and (59) and the dressed-state populations. Equations (58) and (59) are proportional to the decay rates of the dressed states in vacuum. The transitions from a heavily populated dressed state are important.

In Fig. 2, the resonance fluorescences induced by the dipoles $\hat{\mathbf{P}}^{(+)}_{\omega_1}$ and $\hat{\mathbf{P}}^{(+)}_{\omega_2}$ are shown with various values of p_1 and p_2 when the driving field with frequency ω_1 is tuned at the middle point of the two upper levels and the driving field with frequency ω_2 is resonant to the uppermost level. All the curves in Fig. 2 are rescaled to make them have the same height 1.0. The relative heights can be obtained by multiplying the numbers placed near the curves. In these figures, we observe that the central peaks become very sharp as p_1 and p_2 approach unity. The widths of the central peaks could be much smaller than the natural linewidths $2\gamma_1$ and $2\gamma_3$, as shown in Fig. 3. These results can be well understood by the quantum interference discussed in the preceding section. When $p_1=p_2=1$, $\Delta_1=\omega_{12}/2$, and $\Delta_3=0.0$, the steady state of the atom is the nondecaying state $|\varphi_1\rangle$, within which is the total population, and the total fluorescences are completely inhibited via the quantum interference. When p_1 and p_2 depart from unity, there is a certain population in each of the four eigenvectors $|\varphi_1\rangle$, $|\varphi_2\rangle$, $|\varphi_3\rangle$, and $|\varphi_4\rangle$ in the steady state, as shown in Fig. 4. As is well known, the transitions between the same levels of two neighboring manifolds of the dressed states give rise to the central line and the transitions between the different levels of two neighboring manifolds of the dressed states contribute to the sidebands [32(b)]. Therefore, when p_1 and p_2 are not equal to unity, the resonance fluorescence appears and sidebands always exist as shown in Fig. 2, and the four transitions $|\varphi_\sigma\rangle\rightarrow|\varphi_\sigma\rangle$ ($\sigma=1,2,3,4$) always have their contributions to the central lines.

As pointed out in the last part of the preceding section, the constructive quantum interference between the two paths

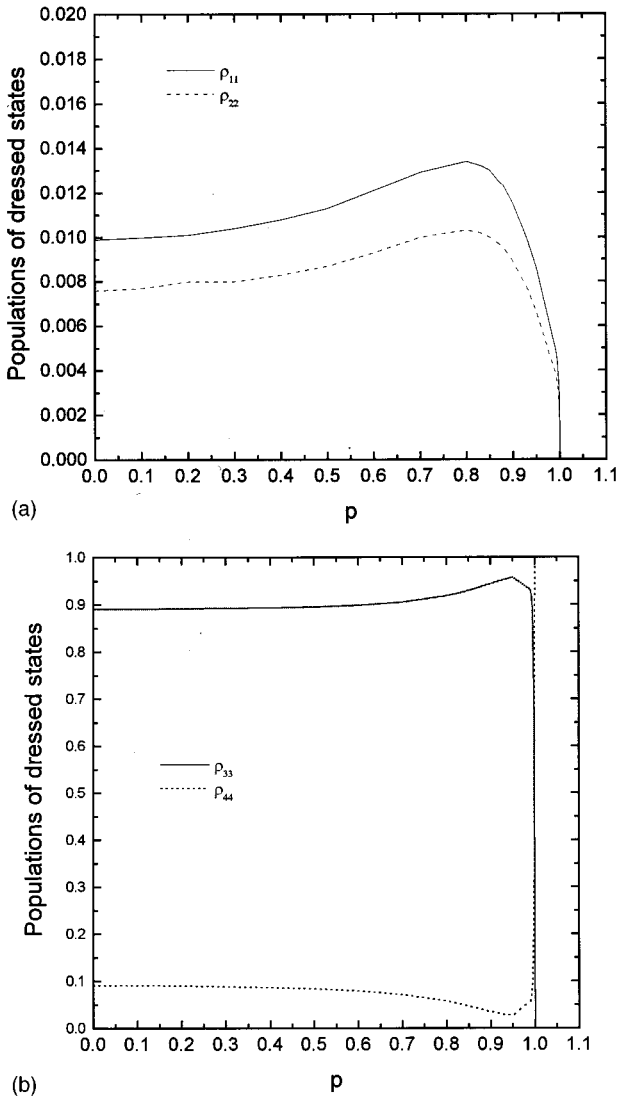

FIG. 4. Dressed state populations (a) ρ_{11} and ρ_{22}; (b) ρ_{33} and ρ_{44} in the steady state versus the parallelism $p(p_1=p_2)$ of the dipole moments with the same parameters as in Fig. 2.

$|a_1\rangle\rightarrow|b\rangle$ (or $|c\rangle$) and $|a_2\rangle\rightarrow|b\rangle$ (or $|c\rangle$) takes action in the transitions $|\varphi_{1,2}\rangle\rightarrow|\varphi_{1,2}\rangle$. The destructive quantum interference plays its role in the transitions $|\varphi_{3,4}\rangle\rightarrow|\varphi_{3,4}\rangle$ but is not sufficiently strong if p_1 and p_2 are not equal to unity [see Eqs. (58) and (59)]. Consequently, the widths of the central lines are not very narrowing, as shown by the curves (a) and (b) of Fig. 2 when p_1 and p_2 are not very close to unity. From Fig. 4(a), we observe that the populations ρ_{11} and ρ_{22} of the dressed states, $|\varphi_1\rangle$ and $|\varphi_2\rangle$, take their maximal values around $p_1=p_2=0.8$, and therefore the sidebands are very pronounced, as shown by the curves (b) of Fig. 2. When p_1 and p_2 approach unity, the population concentrates to $|\varphi_3\rangle$ (or $|\varphi_4\rangle$) as shown in Fig. 4. The main contributions to the central lines come from the transitions $|\varphi_{3,4}\rangle\rightarrow|\varphi_{3,4}\rangle$. Because of the destructive quantum interference in these transitions, the decays of $|\varphi_3\rangle$ and $|\varphi_4\rangle$ are very slow and the central lines become ultranarrow, as shown in Fig. 3 [see Eqs. (58) and (59)]. The two sidebands appearing at ± 0.15 in Fig. 3 are originated from the transitions between $|\varphi_3\rangle$ and $|\varphi_4\rangle$, which can be concluded from the peak positions of the

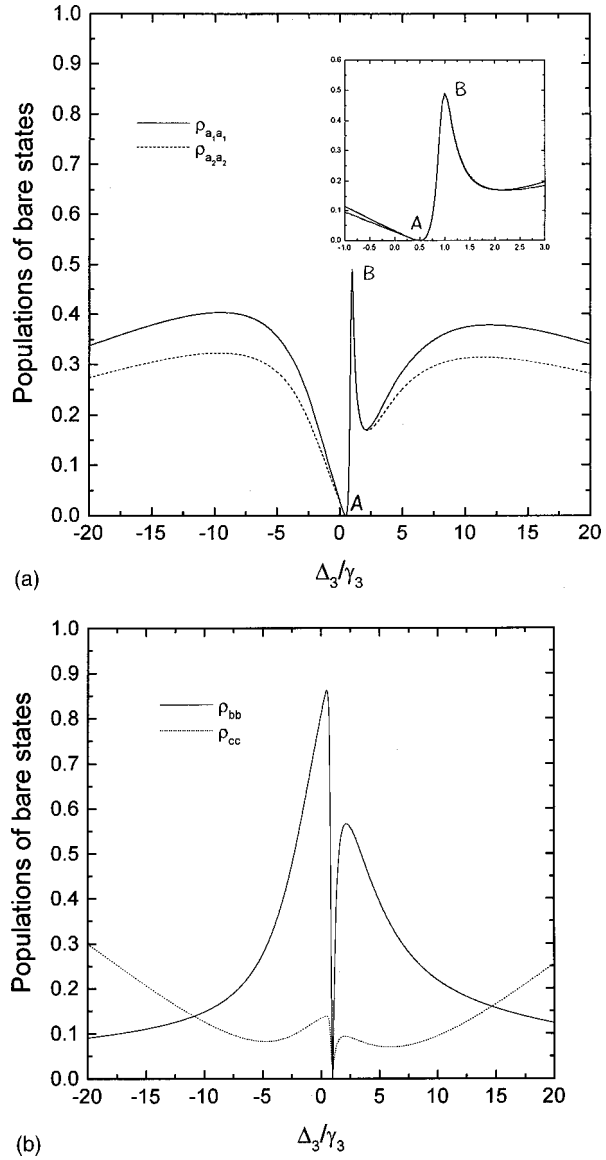

FIG. 5. Bare state populations (a) $\rho_{a_1a_1}$ and $\rho_{a_2a_2}$; (b) ρ_{bb} and ρ_{cc} in the steady state versus the detuning Δ_3 scaled by γ_3 with $\Omega_1=\Omega_2=2.0$, $\Omega_3=\Omega_4=5.0$, $\gamma_1=\gamma_2=0.5$, $\gamma_3=\gamma_4=1.0$, $\omega_{12}=2.0$, $\Delta_1=0.5$, and $p_1=p_2=1.0$.

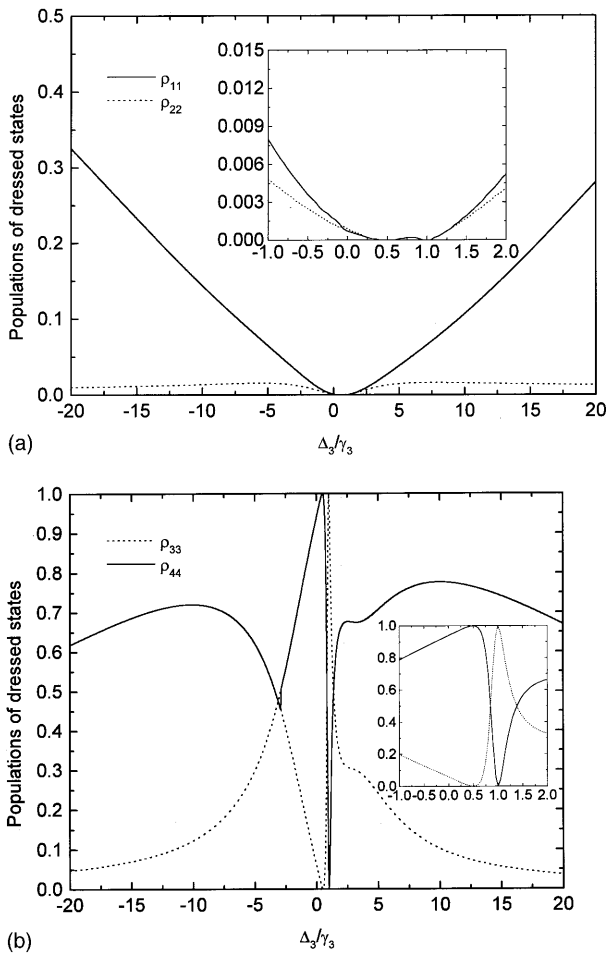

FIG. 6. Dressed state populations (a) ρ_{11} and ρ_{22}; (b) ρ_{33} and ρ_{44} in the steady state versus the detuning Δ_3 scaled by γ_3 with the same parameters as in Fig. 5.

sidebands. For the present parameters, the eigenvalues of $|\varphi_3\rangle$ and $|\varphi_4\rangle$ are 0.1522 and 0.0 (here and in the following we take γ_3 as the unit for decay rates, detunings, and Rabi frequencies), respectively.

The detunings Δ_1 and Δ_3 may be easily adjusted in an experiment. It is more useful to study the effects of varying Δ_1 and Δ_3 on the spectra. When $\Delta_1=\Delta_3\neq\omega_{12}/2$, the steady state of the atom is the dressed state $|\varphi_{III}\rangle$, which means no population in the two upper levels [see point *A* in Fig. 5(a)]. When $\Delta_1\neq\omega_{12}/2$ but $\Delta_3=\omega_{12}/2$, the steady state is the nondecaying state $|\varphi_{II}\rangle$, and a maximum population is in the upper levels [see point *B* in Figs. 5(a)]. If the detuning (Δ_3) is tuned to the neighborhood of the two limits, the populations in the dressed states $|\varphi_1\rangle$ and $|\varphi_2\rangle$ are very small, as shown in Fig. 6(a), and then the contributions from the transitions $|\varphi_{1,2}\rangle\leftrightarrow|\varphi_{1,2}\rangle$ to the central peaks are very small. The central lines are mainly generated by the transitions between $|\varphi_{3,4}\rangle$ and $|\varphi_{3,4}\rangle$. On the other hand, the populations of the two upper levels are nearly equal in this region of Δ_3, as shown in Fig. 5(a). Therefore, the destructive quantum interference in these transitions will be very strong because of $p_1=p_2=1$. In this way, $|\varphi_{3,4}\rangle$ decay very slowly and the central peaks become very sharp, as shown in Figs. 7 and 8. In these figures we plot the spectra for different detunings (Δ_3). It can be seen that for those Δ_3 close to and in the region from $\omega_{12}/2$ to Δ_1, the central peak becomes very sharp and other peaks are depressed almost completely. As Δ_3 increases far away from $\omega_{12}/2$, the dressed states $|\varphi_{1,2}\rangle$ have certain populations in the steady state, as shown in Fig. 6(a). The sidebands and the wider-background emissions appear, as shown by the curves (f) of Figs. 7 and 8. It is interesting that in this case there exist sharp multipeaks on the central wider-background emissions. We notice that as Δ_3 increases, the eigenvalues of the dressed states $|\varphi_3\rangle$ and $|\varphi_4\rangle$ become very close. For example, $\varepsilon_3=-0.5809$ and $\varepsilon_4=-0.2932$ when $\Delta_3=3.0$ and other parameters are the same as in Fig. 7. Because of the destructive quantum interference, the rates of the transitions from $|\varphi_3\rangle\leftrightarrow|\varphi_4\rangle$ are very small. Therefore, these transitions give rise to the very narrowing multipeaks in the central region. When one of p_1 and p_2 or both become zero, the destructive quantum interference disappears and those sharp spectral lines disappear, as shown in Fig. 9. We should emphasize that the ultranarrow spectral

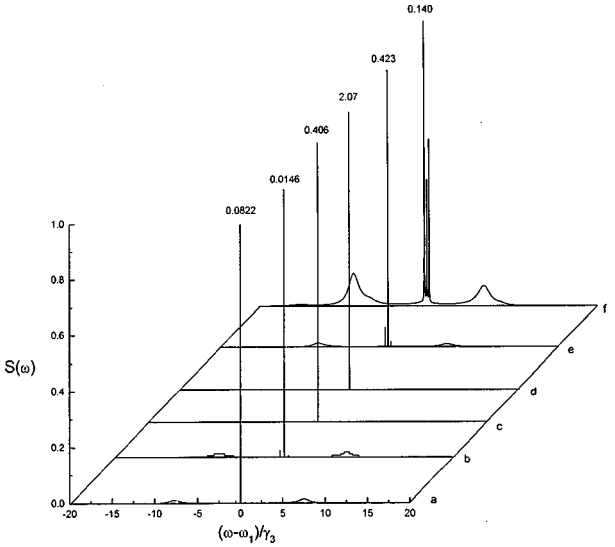

FIG. 7. Resonance fluorescence spectra with the central frequency ω_1 for the parameters $\Omega_1=\Omega_2=2.0$, $\Omega_3=\Omega_4=5.0$, $\gamma_1=\gamma_2=0.5$, $\gamma_3=\gamma_4=1.0$, $\omega_{12}=2.0$, $\Delta_1=0.5$, and $p_1=p_2=1.0$. (a) $\Delta_3=0.0$; (b) $\Delta_3=0.25$; (c) $\Delta_3=0.75$; (d) $\Delta_3=1.25$; (e) $\Delta_3=2.0$; (f) $\Delta_3=3.0$.

lines completely originate from the destructive quantum interference between the decay paths $|a_1\rangle$ and $|a_2\rangle\rightarrow|b\rangle,|c\rangle$, which can be controlled by the parallelism of the dipole polarizations and the difference between Δ_1 and Δ_3. Therefore, for a very wide region of the Rabi frequencies Ω and the upper level separation ω_{12}, not just for the values taken in the above, the narrowing central spectra exist.

V. SUMMARY

We have shown that the resonance fluorescence spectra of the driven four-level atom are greatly modified by the destructive quantum interference between the spontaneous emission pathways from the upper levels to one of the lower levels. The destructive quantum interference can be controlled by the parallelism of the atomic dipole moments and

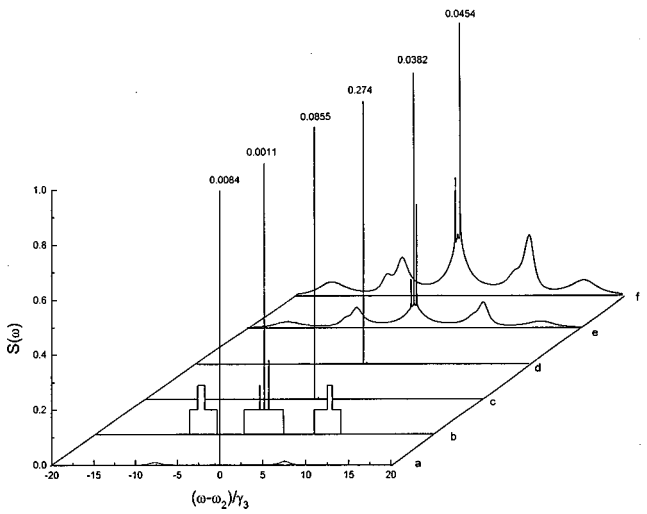

FIG. 8. Resonance fluorescence spectra with the central frequency ω_2. Other notations are the same as Fig. 7.

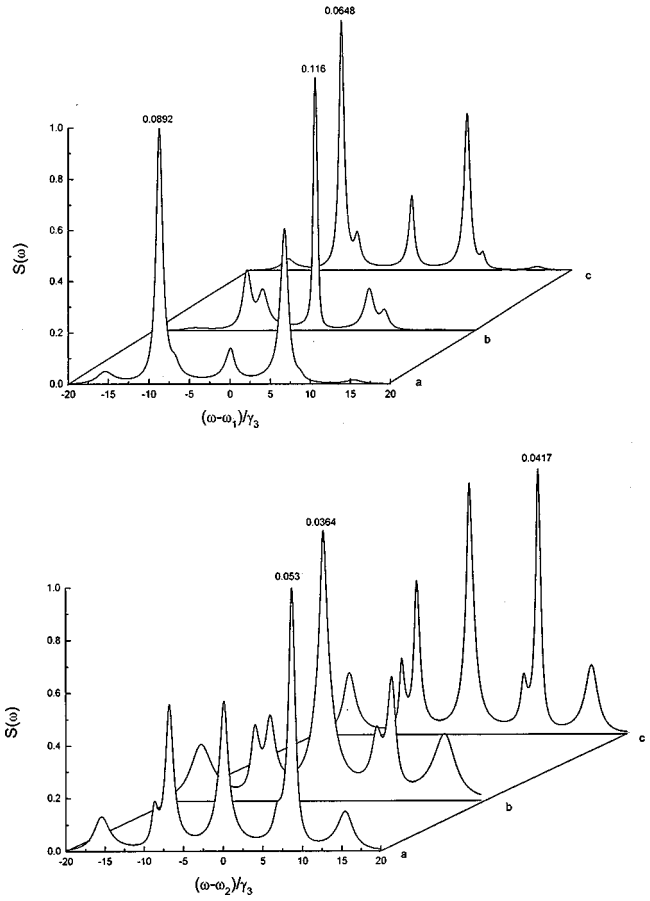

FIG. 9. Resonance fluorescence spectra which is induced by (i) $\hat{\mathbf{P}}^{(+)}_{\omega_1}$, (ii) $\hat{\mathbf{P}}^{(+)}_{\omega_2}$ with $\Omega_1=\Omega_2=2.0$, $\Omega_3=\Omega_4=5.0$, $\gamma_1=\gamma_2=0.5$, $\gamma_3=\gamma_4=1.0$, $\omega_{12}=2.0$, $\Delta_1=0.5$, and $\Delta_3=3.0$. (a) $p_1=1.0$, $p_2=0.0$; (b) $p_1=0.0$, $p_2=1.0$; (c) $p_1=0.0$, $p_2=0.0$.

the detunings of the driving fields. The atom can evolve into a dressed state that is nondecaying and the steady-state fluorescence emitted by the atom is completely suppressed because of the destructive quantum interference when the atomic dipole moments are strictly parallel and one of the driving fields is tuned to the middle point of the upper levels. The fluorescence emissions can also be completely inhibited if the detunings of the two driving fields to the uppermost level are the same. However, this inhibition originates from the population trapping in the lower levels and is irrelevant to the quantum interference between the spontaneous emission pathways. We have also found that the final state of the atom (steady state) depends on the initial atomic condition, when the atomic dipole moments are parallel and both of the driving fields are tuned to the middle point of the upper levels. It is a pure effect of the quantum interference. When the atomic dipole moments are closely but not exactly parallel and one of the driving fields is tuned to the middle point of the upper levels, the destructive quantum interference is not complete. When the atomic dipole moments are strictly parallel but two driving fields depart from the middle point of the upper levels and their detunings are not equal, the destructive quantum interference is also not complete. This incomplete destructive quantum interference leads to very slow decay for one of the dressed states, which exhausts most of the steady-state populations. It is the slow decay that

gives rise to the ultranarrow spectral profile at the line center. The width of the narrow spectral line can be much smaller than the natural linewidth.

For observing the above predicted results in an experiment, we could employ the experimental scheme of Xia *et al.* in sodium dimers [20] with the addition of another laser which couples the upper pair to the lower level ($A\ ^1\Sigma_u^+$). In this experimental scheme, the dipole moments between the upper pair to either of the two lower levels ($A\ ^1\Sigma_u^+$ and $X\ ^2\Sigma_g^+$) are strictly parallel. Therefore, we should observe the predicted effects by varying the detunings of the driving fields and monitoring the resonance fluorescence emitted from the upper pair to the lower level ($A\ ^1\Sigma_u^+$).

ACKNOWLEDGMENTS

This work was supported by HKBU and UGC. F.L.L. also acknowledges support from the National Natural Science Foundation of China.

[1] S. E. Harris, Phys. Rev. Lett. **62**, 1033 (1989).
[2] M. O. Scully, S. Y. Zhu, and A. Gavrielides, Phys. Rev. Lett. **62**, 2813 (1989).
[3] A. Lyras, X. Tang, P. Lambropoulos, and J. Zhang, Phys. Rev. A **40**, 4131 (1989).
[4] O. Kocharovskaya and P. Mandel, Phys. Rev. A **42**, 523 (1990).
[5] A. Imamoglu, Phys. Rev. A **40**, 2835 (1989).
[6] S. E. Harris, J. E. Field, and A. Imamoglu, Phys. Rev. Lett. **64**, 1107 (1990).
[7] K. J. Boller, A. Imamoglu, and S. E. Harris, Phys. Rev. Lett. **66**, 2593 (1991).
[8] K. Hakuta, L. Marmet, and B. P. Stoicheff, Phys. Rev. Lett. **66**, 596 (1991).
[9] P. Mandel and O. Kocharovskaya, Phys. Rev. A **47**, 5003 (1993).
[10] S. R. Wilkinson and A. V. Smith, Quantum Opt. **6**, 317 (1994).
[11] M. O. Scully, Phys. Rev. Lett. **67**, 1855 (1991).
[12] M. O. Scully and S. Y. Zhu, Opt. Commun. **87**, 134 (1992).
[13] M. Fleischhauer *et al.*, Phys. Rev. A **46**, 1468 (1992).
[14] A. S. Zibrov *et al.*, Phys. Rev. Lett. **76**, 3935 (1996).
[15] M. O. Scully and M. Fleischhauer, Phys. Rev. Lett. **69**, 1360 (1992).
[16] S. Y. Zhu, R. C. F. Chan, and C. P. Lee, Phys. Rev. A **52**, 710 (1995).
[17] S. Y. Zhu and M. O. Scully, Phys. Rev. Lett. **76**, 388 (1996).
[18] Hwang Lee, Pavel Polynkin, M. O. Scully, and S.-Y. Zhu, Phys. Rev. A **55**, 4454 (1997).
[19] H. Huang, S. Y. Zhu, and M. S. Zubairy, Phys. Rev. A **55**, 744 (1997).
[20] H. R. Xia, C. Y. Ye, and S. Y. Zhu, Phys. Rev. Lett. **77**, 1032 (1996).
[21] E. Paspalakis and P. L. Knight, Phys. Rev. Lett. **81**, 293 (1998).
[22] D. A. Cardimona, M. G. Raymer, and C. R. Stroud, Jr., J. Phys. B **15**, 55 (1982).
[23] P. Zhou and S. Swain, Phys. Rev. Lett. **77**, 3995 (1996).
[24] P. Zhou and S. Swain, Phys. Rev. A **56**, 3011 (1997).
[25] P. Zhou and S. Swain, Phys. Rev. Lett. **78**, 832 (1997).
[26] B. R. Mollow, Phys. Rev. **188**, 1969 (1969).
[27] L. M. Narducci, M. O. Scully, G.-L. Oppo, P. Ru, and J. R. Tredicce, Phys. Rev. A **42**, 1630 (1990).
[28] A. S. Manka, H. M. Doss, L. M. Narducci, P. Ru, and G.-L. Oppo, Phys. Rev. A **43**, 3748 (1991).
[29] (a) M. Sargent III, M. O. Scully, and W. E. Lamb, Jr., *Laser Physics* (Addison-Wesley, Reading, MA, 1974), Chap. 2, p. 18; (b) Chap. 16, p. 273.
[30] M. Fleischhauer *et al.*, Opt. Commun. **94**, 599 (1992).
[31] M. Lax, Phys. Rev. **129**, 2342 (1963).
[32] (a) M. O. Scully and M. S. Zubairy, *Quantum Optics* (Cambridge University Press, Cambridge, England, 1997), Chap. 7, p. 225; (b) Chap. 10, p. 295.